SOME OBSERVATIONS ON THE INELASTIC ELECTRON-NUCLEON SCATTERING DATA*

M. BREIDENBACH** and J. KUTI***

Laboratory for Nuclear Science and Physics Department, Massachusetts Institute of Technology, Cambridge, Massachusetts 02139, USA

Received 6 April 1972

A compact phenomenological description of the proton data in inelastic electron-nucleon scattering is suggested here. The practical applications of our data analysis are briefly discussed.

Different ideas have been recently introduced to explain the starting findings of the MIT-SLAC collaboration [1]. Less effort has been devoted to several interesting problems from a practical point of view: (i) Sensible Regge phenomenology of inelastic electron-nucleon scattering with its implications for inclusive cross sections in electroproduction. (ii) Problems which require the knowledge of the proton data in the entire kinematic region (as illustration, we mention here the proton polarizability contribution to the hyperfine splitting of the ground state in the hydrogen atom [2,3], and to the Lamb shift in the first excited state [4]. (iii) Tests which require the knowledge of the neutron data, such as the check of the Bloom–Gilman sum rule for the neutron, and evaluation of the neutron-proton mass difference in finite models [5].

We start out with the phenomenological description of the proton data. The observation by Bloom and Gilman [6], which is quantitative in terms of a finite energy sum rule, suggests that the structure function $\nu W_2(q^2, \nu)$ in domain A of fig. 1 may be written as the product of the scaling function $F_2(\omega')$ and a function $R(W)+B(W)$ which oscillates around one at the prominent resonance peaks and becomes one beyond $W \approx 2$ GeV:

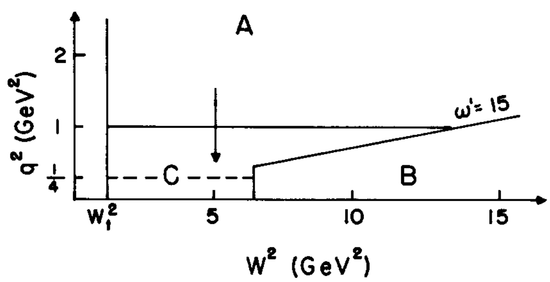

Fig. 1. The kinematic plane in q^2 and W^2. The dashed line indicates the edge of a region in domain C where ansatz (1) of domain A is qualitatively applicable without any modification.

$$\nu W_2(q^2, \nu) = F_2(\omega')\{R(W)+B(W)\}. \tag{1}$$

The invariant mass W of hadrons is related to ν and q^2 by $W^2 = M^2 + 2M\nu - q^2$. We use M = mass of the nucleon, and spacelike values of q^2 are positive, $q^2 = |\boldsymbol{q}|^2 - q_0^2$; $R(W)$ is the sum of relativistic Breit–Wigner forms for the four prominent resonance bumps, and $B(W)$ describes a smooth "background" added to the Breit–Wigner resonances:

$$R(W) = \sum_{i=1}^{4} a_i R_i(W),$$

$$B(W) = 1 - \sum_{i=1}^{3} \frac{b_i}{(1+W-W_t)^i}, \tag{2}$$

where the constants a_i are the amplitudes of the resonance bumps, W_t is the first inelastic pion-nucleon threshold, and the constants b_i denote the parameters

* This work is supported in part through funds provided by the Atomic Energy Commission under Contract AT(11-1)3069.

** Present address: European Organization for Nuclear Research, Geneva.

*** On leave of absence from Eötvös University, Budapest.

of the background form. The degree of the inverse polynomial $B(W)$ can be varied, but background forms with more than three terms have no significant effect on the resonance parameters of the χ^2 of the fits. Notice that $B(W)$ is a smooth function of W which may include some broad N^*-resonances below $W = 2$ GeV.

$R_i(W)$ was parametrized by a resonance mass M_i, and width Γ_i. This form was modified to include the resonance threshold behavior ‡.

For large W above 2 GeV, the resonances are overlapping ($R(W) \to 0, B(W) \to 1$), so that $\nu W_2(q^2,\nu)$ coincides with the scaling function:

$$F_2(\omega') = c_1\left(1-\frac{1}{\omega'}\right)^3 + c_2\left(1-\frac{1}{\omega'}\right)^4 + c_3\left(1-\frac{1}{\omega'}\right)^5 . \quad (3)$$

The simple form (3) has been suggested by the SLAC-MIT collaboration. More rapid approach to scaling behavior has been found in the variable $(2M_\nu+m^2)/q^2$, where m^2 is close to M^2 in the best fits [7] ; $m^2 = M^2$ corresponds to $\omega' = 1 + W^2/q^2$.

For a fixed value of W, the q^2-dependence of $\nu W_2(q^2,\nu)$ in eq. (1) is given by the scaling function $F_2(\omega')$ alone. The ansatz (1) displays the clear oscillations of νW_2 in the low energy resonance region about the scaling limit curve. The prominent resonance bumps remain of the same magnitude as the background and follow in magnitude the height of the scaling limit curve at the corresponding value of the scaling variable ω'.

Eq. (1) represents a satisfactory fit to the data in domain A of fig. 1. In the actual fit we made a cut on the data only in $q^2 : q^2 \geq 1$ GeV^2. Domain A is, however, separated from domain B by the line $\omega' = 15$ (asymptotically we will apply the Regge pole model to the high-energy data). Therefore a few points with $q^2 \geq 1$ GeV^2 and $\omega' = 15$ are included in the fit form domain B, but this is irrelevant.

In the simplest form of the fit $R = 0.18$ was chosen over the entire kinematic region. This choice is a reasonable first approximation to the available data ‡‡ [1]. The parameters of the fit are listed in table 1. The χ^2-test of the fit is $\sqrt{\chi^2/\mathrm{df}} = 1.08$ for 1597 degrees of freedom. Some fits are shown in fig. 2.

The Bloom–Gilman sum rule and its qualitative consequences have indicated that the form (1) would work over a large kinematic region. The sum rule is slightly sensitive to the choice of the scaling variable at least on a level of 10-20%. The statement is true even if scaling is rapid in the corresponding scaling variable [9]. The light cone variable $\omega^L = M/(|\boldsymbol{q}|-q_0)$ is an interesting illustrative example. This variable, and the finite energy sum rules formulated in it, will be discussed in ref. [9] in greater detail.

We notice that ω^L has all the nice qualitative properties. First, scaling in ω^L is better than in ω. The more rapid approach to scaling in ω^L or ω' as compared to ω can be seen by plotting the data in those variables. χ^2-tests confirm this observation. Fitting to the polynomial form (2) in three different variables gives $\sqrt{\chi^2/\mathrm{df}}$-values for 169 degrees of freedom as follows: 1.43 in ω, 1.06 in ω^L, and 0.93 in ω'. This fit was restricted to $W \geq 2$ GeV data points with $\omega' < 2.5$. Second, replacing ω' in eq. (1) by ω^L, the description of resonances and scaling data remains fair (fig. 2). Ansatz (1) in the variable ω^L gives $\sqrt{\chi^2/\mathrm{df}} = 1.14$ for 1597 degrees of freedom in domain A. Third, the difference between the two sides of the Bloom–Gilman sum rule is less than 10%

‡ The resonance shape used for the second, third and forth bumps was

$$R_i = \frac{\Gamma_i^2 M_i^2}{(W^2-M_i^2)^2 + \Gamma_i^2 M_i^2} .$$

For the first resonance, an attempt was made to include threshold effects up to $W = M_1$, in the form

$$R_1(W \leq M_1) = \frac{M}{W}\left(\frac{W^2-M^2}{M_1^2-M^2}\right)^2 \left(\frac{q_*^0}{q_*}\right)^3 \frac{\Gamma_R^2 M_1^2}{(W^2-M_1^2)^2+\Gamma_R^2 M_1^2} ,$$

$$R_1(W > M) = \frac{\Gamma_1^2 M_1^2}{(W^2-M_1^2)^2+\Gamma_1^2 M_1^2} ,$$

where

$$\Gamma_R = \Gamma_1 \frac{V}{V^0}\frac{q_*}{q_*^0}, \qquad V = \frac{(q_* R)^2}{1+(q_* R)^2} ,$$

q_* is the momentum of the decay pion in the isobar rest frame, R is an isobar radius taken to be 0.8 fm, and the 0 superscript implies the corresponding quantity evaluated at $W = M_1$.

‡‡ Across the range $1.1 \leq W \leq 2$ GeV, $R \leq 0.2$ for $0.5 \leq q^2 \leq 2$ GeV^2, and $R \leq 0.35$ for $2 \leq q^2 \leq 4$ GeV^2 has been reported in ref. [8]. $R = \sigma_L/\sigma_T$ is the standard notation.

Table 1
Fit parameters of ansatz (1) with ω'.

i	M_i (GeV)	Γ_i (MeV)	a_i	b_i	c_i
1	1.226	115	0.7178	−0.5291	0.8285
2	1.508	80	0.3999	1.260	1.383
3	1.705	85	0.3268	0.220	−2.003
4	1.920	220	0.0960		

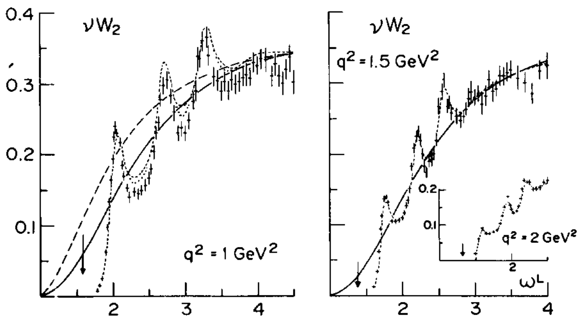

Fig. 2. The function $\nu W_2(q^2, \nu)$ plotted versus $\omega^{\mathrm{L}} = M/(|\boldsymbol{q}| - q_0)$ for fixed q^2-values of 1.0, 1.5 and 2.0 GeV^2. The solid line is the scaling curve $\nu W_2(\omega^{\mathrm{L}})$, a smooth fit to the data in the scaling region. The smooth dashed line, slightly above $\nu W_2(\omega^{\mathrm{L}})$ for $q^2 = 1$ GeV^2, represents the scaling curve in the variable $\omega' = 1 + W^2/q^2$. The short dashed line following the resonances is our ansatz (1) in the variable ω^{L}. The same form (1) from a fit in the variable ω' is very close to the previous one except where dots indicate slight deviation. The arrow shows the position of the elastic peak.

in the light cone variable, for $q^2 \geqslant 1$ GeV^2. However, at $q^2 = 1$ GeV^2 the integrals under the two scaling curves in ω' and ω^{L} respectively, differ by 17% (see fig. 2). With increasing q^2-values this difference is rapidly decreasing.

The tests of the light cone variable ω^{L} indicate that it is a worthy candidate for serving as a natural kinematic variable in other current initiated reactions where the low lying resonances build up the scaling curves through finite energy sum rules.

It will be interesting to see the performance of the form (1) as applied to the neutron data either in ω' or in ω^{L}. The investigation of the deuteron data in the resonance region is in progress at MIT [10]. This study will also allow the test of the Bloom–Gilman sum rule for the neutron data. Such an analysis would provide us with new input to the problem of neutron scaling data close to $\omega' \sim 1$.

In domain B we utilize the high energy description of the data. For fixed q^2 and $W^2/q^2 \gg 1$, we write the conventional form

$$W_2(q^2, \nu) = \beta_{\mathrm{P}}(q^2)\nu^{\alpha_{\mathrm{P}}(0)-2} + \sum_{i=1,2} \beta_i(q^2)\nu^{\alpha_i(0)-2}\,, \quad (4)$$

with a similar expansion for $W_1(q^2, \nu)$. The first term in eq. (4) is the Pomeranchuk trajectory associated with diffractive scattering, the second sum includes the P' ($i = 1$) and A_2 ($i = 2$) trajectories identified with the nondiffractive component of the cross sections. Intercepts $\alpha_{\mathrm{P}}(0) = 1$ and $\alpha_i(0) = \frac{1}{2}$ are chosen here. We have found it rather ad hoc to introduce additional low lying trajectories with negative intercepts [11] which are not appealing for simple phenomenology. The motivations of ref. [11] to introduce negative intercepts are also disputable [9].

There is the kinematic constraint on the residue functions that $W_2(q^2, \nu)$ vanishes in the limit $q^2 \to 0$. The residue functions satisfy a spectral representation in q^2 [9, 12] which incorporates this kinematic condition. For positive q^2, the spectral representation motivates a simple form for the residue functions:

$$\beta_{\mathrm{P}}(q^2) = C_{\mathrm{P}} \frac{q^2}{q^2 + \mu^2}\,,$$

$$\beta_i(q^2) = C_i \frac{q^2}{\sqrt{2M(q^2 + \mu^2)}}\,,$$

where μ^2 is a mass parameter characterizing the q^2-dependence of the residue functions. An analogous expression with a mass parameter m^2 can be written for the residue functions of $W_1(q^2, \nu)$. The same characteristic mass μ was chosen in all terms in (5). We feel that present data do not suggest more sophistication, but the refinements required by more accurate data will be interesting. The parameter μ should not be identified with m_ρ. We use the form (5) for smooth interpolation in the spacelike region which is not suitable for continuation to timelike q^2-values.

Eq. (4) together with (5) represents the simplest interpolation between the photoproduction limit and the scaling region. It is based on the plausible assumption that both components of (4) scale in the appropriate kinematic region. Our Regge pole model is discussed theoretically in refs. [9, 13].

$R = \sigma_L/\sigma_T$ is explicit function of q^2 and ν with the parameters introduced in the two structure functions. For the simplest illustration we take here $m^2 = \mu^2$ which corresponds to $R = q^2/\nu^2$. More detailed discussion on R will be given in ref. [9]. Introducing the variable $\omega^R = 2M\nu/(\mu^2+q^2)$, we write (4) as

$$(1+\mu^2/q^2)\nu W_2(q^2,\nu) = C_P + \sum_{i=1,2} C_i/\sqrt{\omega^R}\,. \qquad (6)$$

Eq. (6) displays scaling manifestly when q^2 is large.

The best fit to the most accurate new 6° data [1] gives $C_P = 0.26$, $C_1+C_2 = 0.36$, $\mu^2 = 0.25\ \mathrm{GeV}^2$. The sorting conditions $W > 2.5$ GeV and $\omega > 10$ have been introduced in the fit. The χ^2 test gives $\sqrt{\chi^2/\mathrm{df}} = 0.82$ for 32 data points. Including the 1.5° data and the old 6° and 10° data in the fit (with the same sorting conditions), the parameters slightly change, but the fit is still satisfactory: $\sqrt{\chi^2/\mathrm{df}} = 1.11$ for 116 data points. All the reasonable fits to different data sets [9] are in the range $C_P = 0.26 \pm 0.05$, $C_1+C_2 = 0.36 \pm 0.1$, $\mu^2 = 0.25 \pm 0.05\ \mathrm{GeV}^2$.

The form (6) represents a smooth interpolation between the photoabsorption limit and scaling data (fig. 3). The photoabsorption cross section is $\sigma(\nu) = (117+54/\sqrt{\nu})\mu\nu$ in our fit with ± 10–20% statistical and systematic uncertainty.

Some remarks are appropriate here. First, we made a cut on the data at $\omega = 10$, however a shift to $\omega' = 15$ has no noticeable influence of the results. At $q^2 = 0$, the $\nu = 2$ GeV point corresponds to $\omega^R \simeq 15$. About 30% of the scaling function is nondiffractive in that region, and an asymptotic Regge behavior may well set in around here (it is imporper to compare, say $\nu = 6$ GeV in real photoabsorption to $\omega = 6$ in the scaling region). Second, if the value of μ turns out to be the same for the neutron, and we emphasize that it has not been checked, then from the total photoabsorption data on deuterium target we can separate C_1 and C_2 in our fit [15]: $C_1/C_2 \simeq 4.4$. Third, if factorization holds at high energies, the characteristic

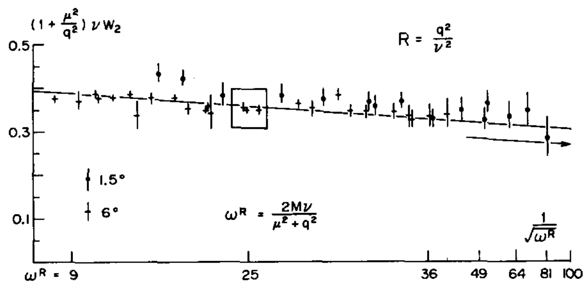

Fig. 3. The function $(1+\mu^2/q^2)\nu W_2$ plotted versus $\omega^R = 2M\nu/(\mu^2+q^2)$. The solid line is the Regge form (6) from a fit to the most accurate 6° data. Some 1.5° and 6° data are plotted here. To show the smooth interpolation of (6) in q^2, three data points are framed in the figure around $\omega^R = 25$ with q^2-values 0.15, 0.68 and 0.85 GeV^2. The arrow indicates the fit to photoproduction data of bubble chamber and counter experiments (see ref. [15]).

parameter to describe the shrinking photon and the rapid approach to scaling for $\omega \gg 1$ is given by $\mu^2 \simeq 0.25\ \mathrm{GeV}^2$, the same value for *different* target particles.

Domain C of fig. 1 is easily approximated by smooth interpolation from domains A and B. In fact, the form (1) works qualitatively down to $q^2 = 0.25\ \mathrm{GeV}^2$, well inside region C [9].

Finally, we list some applications of the data analysis. Our Regge pole model when combined with the hypothesis of factorization has been used to get estimates on inclusive electroproduction from nucleons when the fragment of the nucleon is detected in the final state [9, 16]. From the analysis of Gàlfi and Hasenfratz [16], we conclude that the structure functions of the inclusive process with a target fragment in the final state would scale in the form as conjectured in the light cone algebra of currents and the parton model. An interesting test of the Regge pole model has been suggested [9, 17] by detecting the influence of q^2 on the average transverse momentum of the slow fragment particle.

Gnädig [2] has derived upper and lower bounds in terms of $W_1(q^2,\nu)$ and $W_2(q^2,\nu)$ on the unknown part of the proton polarizability (denoted by $\delta_P(\Delta_2)$ in ref. [3]) to the hyperfine splitting in the ground state of the hydrogen atom. He finds from our data analysis upper and lower bounds on δ_1 which are in agreement with the Rafael's numerical results in ref. [3] *. The problem of the hyperfine structure is discussed in great detail by Gnädig and Kuti [2].

A similar parametrization of the neutron data will allow us to test the contribution of the resonance region and the large ν-low q^2 region to the neutron-proton mass difference in finite theoretical models. These two regions have been ignored in a previous calculation [5].

The authors would like to express their deep appreciation for help, stimulation and criticism to R. Brandt, J. Friedman, F. Gilman, H. Kendall, G. Marx. M. Nauenberg, F. Niedermayer and V.F. Weisskopf. We thank the members of the SLAC-MIT collaboration for many helpful discussions.

* The authors of ref. [2] acknowledge Dr. de Rafael's criticism who has pointed out an error in the numerical calculations of ref. [2].

References

[1] For a review of the kinematics and the experimental aspects of inelastic electron-nucleon scattering, see H.W. Kendall, Invited talk in the Proceedings of the 1971 International Symposium on Electron and Photon Interactions at High Energies, Cornell University, Ithaca, August 23-27 (1971).

[2] P. Gnädig, Eötvös University Thesis; P. Gnädig and J. Kuti, to be published.

[3] E. de Rafael, Phys. Letters 37B (1971) 201.

[4] E. Gajzágó, private communication.

[5] T.D. Lee, Invited talk given at the Amsterdam International Conference onElementary Particles (1971).

[6] E.D. Bloom and F.J. Gilman, Phys. Rev. Letters 25 (1970) 1140; E.D. Bloom and F.J. Gilman, Phys. Rev. D4 (1971) 2901. For a different approach within the framework of the resonance model, see, for example, G. Domokos, S. Kovesi–Domoskos and E. Schonberg, Phys. Rev. D3 (1971) 1184.

[7] G. Miller et al., Phys. Rev. D5 (1972).

[8] F.W. Brasse et al., DESY Report (1970).

[9] M. Breidenbach and J. Kuti (in preparation), in which an exhaustive account of the results of this letter will be published.

[10] J. Friedman, private communication.

[11] F. Close and J. Gunion, Phys. Rev. D4 (1971) 742.

[12] H. Pagels, Phys. Letters 34B (1971) 299.

[13] R. Brandt, M. Breidenbach and P. Vinciarelli, University of Maryland (1971).

[14] E. Bloom et al., to be published.

[15] G. Wolf, Proceedings of the 1971 International Symposium on Electron and Photon Interactions at High Energies, Cornell University, Ithaca, August 23-27 (1971).

[16] L. Gàlfi and P. Hasenfratz, Nuovo Cimento Letters (in press).

[17] H. Abarbanel and J. Kogut, Institute for Advanced Study preprint (1971).